

Effects of in-medium nucleon-nucleon cross section on collective flow and nuclear stopping in heavy-ion collisions in the Fermi-energy domain

Pengcheng Li,^{1,2} Yongjia Wang^{*},¹ Qingfeng Li^{†,1,3} Chenchen Guo,⁴ and Hongfei Zhang²

¹*School of Science, Huzhou University, Huzhou 313000, China*

²*School of Nuclear Science and Technology, Lanzhou University, Lanzhou 730000, China*

³*Institute of Modern Physics, Chinese Academy of Sciences, Lanzhou 730000, China*

⁴*Sino-French Institute of Nuclear Engineering and Technology, Sun Yat-sen University, Zhuhai 519082, China*

(Dated: September 22, 2018)

With the newly updated version of the ultrarelativistic quantum molecular dynamics (UrQMD) model, a systematic investigation of the effects of in-medium nucleon-nucleon (NN) elastic cross section on the collective flow and the stopping observables in $^{197}\text{Au} + ^{197}\text{Au}$ collisions at beam energies from 40 to 150 MeV/nucleon is performed. Simulations with the medium correction factor $\mathcal{F} = \sigma_{NN}^{\text{in-medium}}/\sigma_{NN}^{\text{free}} = 0.2, 0.3, 0.5$, and the one obtained with the FU3FP1 parametrization which depends on both the density and the momentum are compared to the FOPI and INDRA experimental data. It is found that, to best fit the experimental data of the slope of the directed flow and the elliptic flow at mid-rapidity as well as the nuclear stopping, the correction factor $\mathcal{F}=0.2$ and 0.5 are required for reactions at beam energies of 40 and 150 MeV/nucleon, respectively. While calculations with the FU3FP1 parametrization can simultaneously reproduce these experimental data reasonably well. And, the observed increasing nuclear stopping with increasing beam energy in experimental data can also be reproduced by using the FU3FP1 parametrization, while the calculated stopping power in Au+Au collisions with beam energies from 40 to 150 MeV/nucleon almost keeps constant when take \mathcal{F} equal to a fixed value.

PACS numbers: 25.70.-z, 21.65.Mn, 25.75.Ld

I. INTRODUCTION

Investigations of the equation of state (EoS) of nuclear matter and the nucleon-nucleon (NN) cross section have drawn much attention during the past several decades in both nuclear physics and astrophysics due that they are essential for understanding many phenomena in nuclear structures and reactions, as well as in astrophysical nuclear processes [1–5]. So far, the stiffness of the EoS for isospin symmetric nuclear matter has been relatively well understood, though there still remains some uncertainties for further improvement [6–9]. Concerning the NN cross section, in free space, its information has been well measured by experiments, but in the nuclear medium, it should be relied on comparison of the theoretical calculations to experimental data of heavy ion collisions (HICs). It is well known that the in-medium NN cross section is suppressed when compared to the free one, however, the degree of this suppression is still far from being completely pinned down.

Theoretically, the in-medium NN cross section can be calculated by using different methods, e.g., the Dirac-Brueckner approach with the Bonn potential [10], the Dirac-Brueckner-Hartree-Fock approach with realistic nucleon-nucleon potential [11], the relativistic Brueckner-Hartree-Fock model [12–14], the T-matrix approach [15, 16], and the relativistic BUU (RBUU) microscopic trans-

port theory with the effective Lagrangian [17, 18]. Alternatively, the detailed information of the in-medium NN cross section can be deduced from the comparison of observables of HICs with corresponding transport model simulations. For instance, by studying the balance energy, the collective flow and the stopping power with microscopic transport models, strong evidence for the reduction of NN cross section in nuclear medium have been confirmed in HICs at intermediate energies [19–36]. The frequently used transport models for the HICs at low and intermediate energies are the Quantum Molecular Dynamics (QMD) model [37] and the Boltzmann- (Vlasov) Uehling-Uhlenbeck (BUU, VUU) model [38]. Usually, parameterized in-medium NN elastic cross sections are adopted in transport model for simplicity. For example, $\sigma_{NN}^{\text{in-medium}} = (1 - \eta\rho/\rho_0)\sigma_{NN}^{\text{free}}$ with $\eta = 0.2$ has been used in models and it was found to better reproduce the flow and stopping experimental data [20, 28]. In the pBUU model, the in-medium NN cross section is implemented in the form $\sigma_{NN}^{\text{in-medium}} = 0.85\rho^{-2/3}/\tanh(\frac{\sigma_{NN}^{\text{free}}}{0.85\rho^{-2/3}})$ [30]. While in the isospin-dependent Boltzmann-Uehling-Uhlenbeck (IBUU) model and the Lanzhou Quantum Molecular Dynamics (LQMD) model, the in-medium NN cross section is reduced by a factor $\mathcal{F} = \sigma_{NN}^{\text{in-medium}}/\sigma_{NN}^{\text{free}} = (\mu_{NN}^*/\mu_{NN})^2$, where μ_{NN}^* and μ_{NN} are the k -masses of the colliding nucleon partners in the nuclear medium and in free space [26, 32], respectively. In Ref. [36], the ratio between the mean squared rapidity variances in the impact parameter direction and in the longitudinal direction $R = \frac{\langle y_n^2 \rangle}{\langle y_z^2 \rangle}$ as a function of the charge number of the fragments produced in Au+Au collisions at 150

*corresponding author: wangyongjia@zjhu.edu.cn

†corresponding author: liqf@zjhu.edu.cn

MeV/nucleon was investigated, the global trend with increasing charge number can be reproduced by the “standard” QMD model (of J. Aichelin *et al.*) in which the free NN cross section is considered. However, the calculated R of $Z=1$ fragments is much larger than the measured data, which also implies that a reduction in the NN cross section might be necessary. Hence, the NN cross section in different transport models behaves differently and deserves further investigation.

Recently, a systematic study of nuclear stopping of protons from central HICs at Fermi-energy domain was performed by the INDRA collaboration using the powerful INDRA 4π array, it was demonstrated that the mean free path $\lambda_{NN}=9.5\pm 2$ fm at the beam energy of 40 MeV/nucleon and $\lambda_{NN}=4.5\pm 1$ fm at 100 MeV/nucleon, based on the assumption that $\sigma_{NN} \approx 1/(\rho\lambda_{NN})$, the correction factor $\mathcal{F} = \sigma_{NN}^{\text{in-medium}}/\sigma_{NN}^{\text{free}}$ is then deduced to be 0.16 ± 0.04 at 40 MeV/nucleon and 0.5 ± 0.06 at 100 MeV/nucleon, respectively [39]. These stopping data provide a new opportunity to re-visit the in-medium NN cross section by using transport models [40–43]. In our previous works, within the ultrarelativistic quantum molecular dynamics (UrQMD) model, it is found that the collective flow of light clusters and the nuclear stopping can be reproduced reasonable well with the consideration of a medium correction factor \mathcal{F} (which depends on density and momentum) on the free NN cross section [44–46]. Thus, it is of great interest to know the difference between the \mathcal{F} extracted from experimental data [39] and the one adopted currently in the UrQMD model.

In this work, with the updated potential version of the UrQMD model, we investigate the influence of the in-medium NN cross section on collective flow and stopping of protons from Au+Au collisions at Fermi-energy domain by considering various corrections. In the next section the UrQMD model, the in-medium correction factors of NN elastic cross section, as well as flow and stopping quantities are introduced briefly. In Sec. III, effects on both observables of free protons and hydrogen isotopes are shown and discussed. Finally, a summary is given in Sec. IV.

II. MODEL DESCRIPTION AND OBSERVABLES

In the UrQMD model, each nucleon is represented by Gaussian wave packet with the width parameter L in phase space [47]. Usually, $L = 2$ fm² is chosen for simulating Au+Au collisions. The centroids of coordinate \mathbf{r}_i and momentum \mathbf{p}_i of nucleon i are propagated according to

$$\dot{\mathbf{r}}_i = \frac{\partial \langle H \rangle}{\partial \mathbf{p}_i}, \quad \dot{\mathbf{p}}_i = -\frac{\partial \langle H \rangle}{\partial \mathbf{r}_i}. \quad (1)$$

Here, $\langle H \rangle$ is the total Hamiltonian function of the system, it comprises the kinetic energy T and the effective interaction potential energy U . For studying HICs at

intermediate energies, the following density and momentum dependent potential was frequently used in QMD-like models [37, 46, 48],

$$U = \alpha \cdot \left(\frac{\rho}{\rho_0}\right) + \beta \cdot \left(\frac{\rho}{\rho_0}\right)^\gamma + t_{md} \ln^2 [1 + a_{md} (\mathbf{p}_i - \mathbf{p}_j)^2] \frac{\rho}{\rho_0}. \quad (2)$$

Here $\alpha = -393$ MeV, $\beta = 320$ MeV, $\gamma = 1.14$, $t_{md} = 1.57$ MeV, and $a_{md} = 0.0005$ MeV⁻² are chosen, which yields the incompressibility $K_0 = 200$ MeV for isospin symmetric nuclear matter. In recent years, to better describe the recent experimental data at intermediate energies and following present progress on determining the nuclear symmetry energy, the surface, and surface asymmetry energy term, as well as the bulk symmetry energy term obtained from the Skyrme potential energy density functional have been further introduced to the present version [45, 49], which reads as

$$\begin{aligned} u_{\text{Skyrme}} &= u_{\text{sur}} + u_{\text{sur,iso}} + u_{\text{sym}} \\ &= \frac{g_{\text{sur}}}{2\rho_0} (\nabla \rho)^2 + \frac{g_{\text{sur,iso}}}{2\rho_0} [\nabla(\rho_n - \rho_p)]^2 \\ &\quad + \left(A_{\text{sym}} \frac{\rho^2}{\rho_0} + B_{\text{sym}} \frac{\rho^{\eta+1}}{\rho_0^\eta} + C_{\text{sym}} \frac{\rho^{8/3}}{\rho_0^{5/3}} \right) \delta^2. \end{aligned} \quad (3)$$

Here, $\delta = (\rho_n - \rho_p)/(\rho_n + \rho_p)$ is the isospin asymmetry defined by the neutron (ρ_n) and proton (ρ_p) densities. And, the parameters g_{sur} , $g_{\text{sur,iso}}$, A_{sym} , B_{sym} , and C_{sym} are related to the Skyrme parameters via

$$\frac{g_{\text{sur}}}{2} = \frac{1}{64} (9t_1 - 5t_2 - 4x_2 t_2) \rho_0, \quad (4)$$

$$\frac{g_{\text{sur,iso}}}{2} = -\frac{1}{64} [3t_1(2x_1 + 1) + t_2(2x_2 + 1)] \rho_0, \quad (5)$$

$$A_{\text{sym}} = -\frac{t_0}{4} (x_0 + 1/2) \rho_0, \quad (6)$$

$$B_{\text{sym}} = -\frac{t_3}{24} (x_3 + 1/2) \rho_0^\eta, \quad (7)$$

$$C_{\text{sym}} = \frac{1}{24} \left(\frac{3\pi^2}{2}\right)^{2/3} \rho_0^{5/3} \Theta_{\text{sym}}, \quad (8)$$

where $\Theta_{\text{sym}} = 3t_1 x_1 - t_2(4 + 5x_2)$ [45]. In this work, the SV-sym34 force, in which $g_{\text{sur}} = 18.2$ MeV fm², $g_{\text{sur,iso}} = 8.9$ MeV fm², $A_{\text{sym}} = 20.3$ MeV, $B_{\text{sym}} = 14.4$ MeV, and $C_{\text{sym}} = -9.2$ MeV, and the slope parameter of the symmetry energy $L = 80.95$ MeV, is employed.

The directed v_1 and elliptic v_2 flows are the two of most frequently studied observables in HICs, which can be deduced from the Fourier expansion of the azimuthal distribution of detected particles [50], and reads as,

$$v_1 \equiv \langle \cos(\phi) \rangle = \left\langle \frac{p_x}{p_t} \right\rangle, \quad (9)$$

$$v_2 \equiv \langle \cos(2\phi) \rangle = \left\langle \frac{p_x^2 - p_y^2}{p_t^2} \right\rangle, \quad (10)$$

in which p_x and p_y are the two components of the transverse momentum $p_t = \sqrt{p_x^2 + p_y^2}$. And the angle brackets in Eq.9 and Eq.10 indicate an average over all considered particles from all events. Besides the directed and elliptic flows, the nuclear stopping power which characterizes the transparency of the colliding nuclei is another important observable and can be defined with different quantities. A possible measurement of the degree of stopping is $vartl$ (proposed by the FOPI collaboration [50]) which is defined as the ratio of the variances of the transverse to those of the longitudinal rapidity distribution, reads as,

$$vartl = \frac{\langle y_x^2 \rangle}{\langle y_z^2 \rangle}, \quad (11)$$

here

$$\langle y_{x,z}^2 \rangle = \frac{\sum (y_{x,z}^2 N_{y_{x,z}})}{\sum N_{y_{x,z}}}, \quad (12)$$

where $\langle y_x^2 \rangle$ and $\langle y_z^2 \rangle$ are the variances of the rapidity distributions of particles in the x and z directions, respectively. Another quantity R_E is also used to measure the stopping power, which was proposed by the INDRA collaboration, and defined as the ratio of transverse to parallel energy, reads as,

$$R_E = \frac{\sum E_{\perp}}{2 \sum E_{\parallel}}, \quad (13)$$

where E_{\perp} (E_{\parallel}) is the transverse (parallel) kinetic energy of particles in center-of-mass system [51]. Apparently, one can expect that for full stopping, both R_E and $vartl$ values will be unity, while they will be zero for full transparency.

The in-medium NN elastic cross section is treated to be factorized as the product of a medium correction factor $\mathcal{F}(\rho, p)$ and the free cross section and reads,

$$\sigma_{NN}^{\text{in-medium}} = \mathcal{F}(\rho, p) * \sigma_{NN}^{\text{free}} \quad (14)$$

with

$$\mathcal{F}(\rho, p) = \frac{\lambda + (1 - \lambda)e^{-\rho/\rho_0/\zeta} - f_0}{1 + (p_{NN}/p_0)^{\kappa}} + f_0. \quad (15)$$

Where p_{NN} is the relative momentum of two colliding nucleons. In this work, the $\lambda = 1/3$, $\zeta = 1/3$, $f_0 = 1$, $p_0 = 0.425$ GeV/ c , and $\kappa = 5$, which corresponds to the FU3FP1 parametrization used in Ref. [44]. In addition, if p_{NN} is larger than 1 GeV/ c , $\mathcal{F}(\rho, p)$ is set to be unity.

The in-medium correction factor $\mathcal{F}(\rho, p)$ obtained from the FU3FP1 parametrization is displayed in Fig.1, as functions of both reduced density ρ/ρ_0 and momentum p (here $p = p_{NN}$). It is seen that values of \mathcal{F} obtained within ($0.3 \leq \rho/\rho_0 \leq 1.5$, $0 \leq p \leq 0.4$ GeV/ c) cover the results obtained from Ref. [39]. In order to evaluate the effect of \mathcal{F} values from the FU3FP1 parametrization and suggested in Ref. [39] on flow parameters and nuclear stopping discussed above, three fixed in-medium correction factors $\mathcal{F} = 0.2, 0.3$, and 0.5 are further considered for this work.

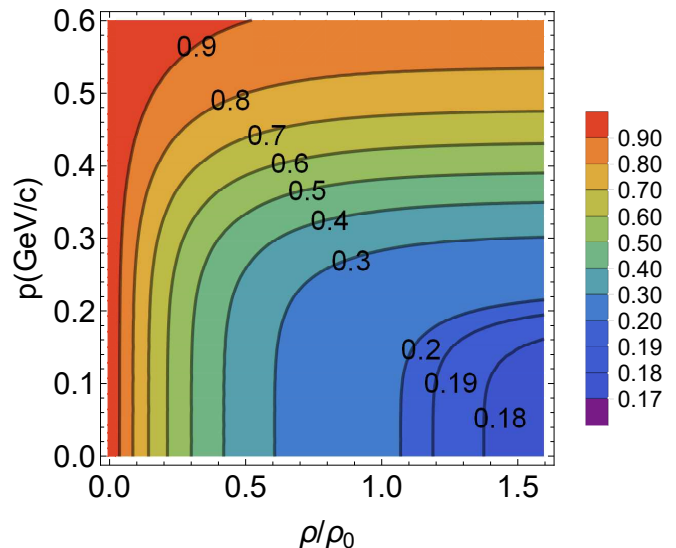


FIG. 1: (Color online) The in-medium correction coefficient \mathcal{F} obtained from the FU3FP1 parametrization as functions of density and momentum.

III. RESULTS AND DISCUSSIONS

In order to have enough statistics for the analysis of the result, more than 450 thousand Au+Au events within the impact parameter $b = 0 - 7.5$ fm at each beam energy (40, 50, 60, 80, 90, 100, 120, or 150 MeV/nucleon) are simulated. An isospin-dependent minimum span tree algorithm (iso-MST) is used to recognize fragments. Nucleons with relative distances smaller than R_0 and relative momenta smaller than P_0 are considered to belong to the same cluster. With proper set of these parameters, fragment mass distribution in intermediate energies HICs can be reproduced [52–54]. In the present work, R_0 and P_0 are set to $R_0^{pp} = 2.8$ fm, $R_0^{nn} = R_0^{np} = 3.8$ fm and $P_0 = 0.25$ GeV/ c . Although the (iso-)MST method has been widely used in transport model to recognize fragments, the values of these coalescence model parameters (R_0 and P_0) are different in different models, see e.g., Refs. [31, 37, 53–55, 57]. Meaningful constraint on the in-medium NN cross section can be extracted from transport calculations only if these parameters which are not under full control do not apparently affect the observable of interest. It was found that the influence of the coalescence model parameters on the collective flow of free protons is relatively weak, see e.g., Refs. [45, 58]. In Ref. [55], the influence of coalescence model parameters on the degree of nuclear stopping was studied, with a maximum set of these parameters, the $vartl$ for $Z=1-6$ particles obtained with iso-MST is about 7% larger than that with the isospin-independent MST. Thus in this work, only the collective flow and nuclear stopping of free protons are used to extract the in-medium NN cross section.

A. Collective flow

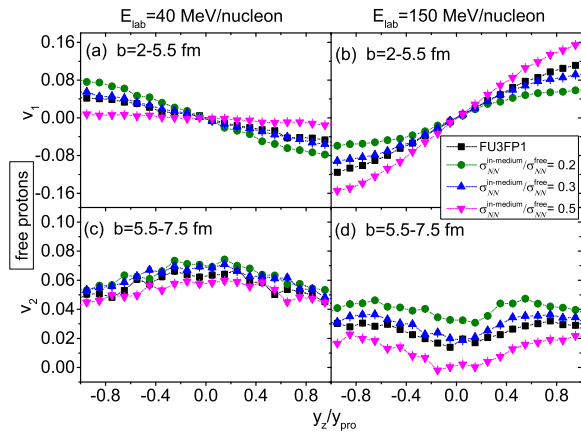


FIG. 2: (Color online) The directed flow v_1 and elliptic flow v_2 of free protons from Au+Au collisions at $E_{lab} = 40$ (left panels) and 150 MeV/nucleon (right panels), as a function of the reduced rapidity y_z/y_{pro} . The impact parameters are chosen to be $b=2-5.5$ fm and $b=5.5-7.5$ fm for the directed and elliptic flows, respectively. The calculations performed with the in-medium correction factors $\mathcal{F} = 0.2$ (circles), $\mathcal{F} = 0.3$ (up-triangles), and $\mathcal{F} = 0.5$ (down-triangles) are compared with calculations using the FU3FP1 parametrization on the in-medium NN cross section (squares).

Fig.2 shows the directed (v_1) and elliptic (v_2) flows of free protons as a function of the reduced longitudinal rapidity (y_z/y_{pro}) from $^{197}\text{Au} + ^{197}\text{Au}$ collisions at 40 MeV/nucleon and 150 MeV/nucleon with different medium correction factors (\mathcal{F}). It can be clearly seen that both v_1 and v_2 are affected by the medium correction factor \mathcal{F} . The difference in v_1 or v_2 with different \mathcal{F} becomes more evident at $E_{lab} = 150$ MeV/nucleon than that at 40 MeV/nucleon, because at the higher beam energy one expects that the collision term plays the more important role. Further, the value of slope of v_1 at mid-rapidity ($y_z/y_{pro}=0$) increases and the value of v_2 at $y_z/y_{pro}=0$ decreases with increasing \mathcal{F} . This is due to the fact that the increasing collision number makes nucleons more likely undergo a bounce-off (positive v_1 slope) motion and squeeze-out (negative v_2) pattern. In addition, it is interesting to see that both the v_1 and v_2 obtained with the FU3FP1 are very close to that obtained with $\mathcal{F} = 0.3$.

To quantitatively estimate the influence of the medium correction factor on the directed flow and elliptic flow, the v_1 slope value and the v_2 value at mid-rapidity for hydrogen isotopes calculated with different \mathcal{F} values are compared to the FOPI and INDRA experimental data taken from Ref. [56], and shown in Fig. 3. Similar to the results shown in Fig. 2, the value of v_1 slope increases and the value of v_2 decreases with increasing E_{lab} . Once again, the results obtained with the FU3FP1 and with

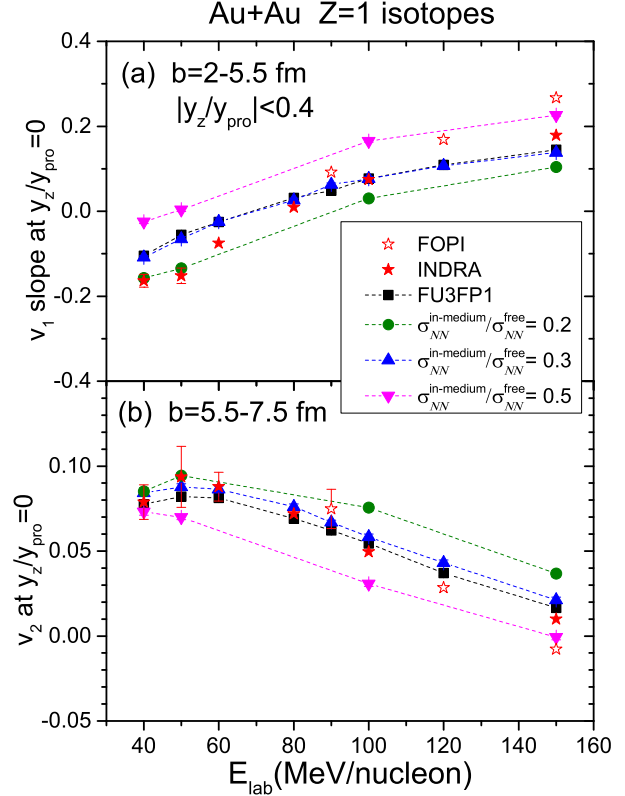


FIG. 3: (Color online) Beam energy dependence of v_1 slope [panel (a)] and v_2 [panel (b)] at mid-rapidity for hydrogen isotopes from $^{197}\text{Au} + ^{197}\text{Au}$ collisions. The chosen impact parameters are $b=2-5.5$ fm and $b=5.5-7.5$ fm for v_1 and v_2 , respectively. The v_1 slope is obtained with assuming $v_1(y_0) = v_{11}y_0 + v_{13}y_0^3 + c$ in the range of $|y_0| = |y_z/y_{pro}| < 0.4$. Calculated results with four in-medium correction factors are presented by different lines as indicated, the FOPI experimental data (open stars) and the INDRA experimental data (solid stars) are taken from Ref. [56].

$\mathcal{F} = 0.3$ overlap appreciably in the whole beam energy region. And, as a whole, the FU3FP1 and $\mathcal{F} = 0.3$ cases best describe the experimental data among all calculations. It is also seen that, both the v_1 and v_2 observables can be reproduced well with $\mathcal{F} = 0.2$ at $E_{lab} = 40$ MeV/nucleon. While, at $E_{lab} = 150$ MeV/nucleon, calculations with $\mathcal{F} = 0.5$ lie between the FOPI and the INDRA experimental data. Therefore, our calculations on the \mathcal{F} factor are quite similar to the results shown in Ref. [39].

To understand more clearly the difference caused by different medium correction factors on the collective flow, the transverse momentum p_t dependence of the parameters v_1 and v_2 of free protons from $^{197}\text{Au} + ^{197}\text{Au}$ collisions at $E_{lab} = 150$ MeV/nucleon are exhibited in Fig. 4. First of all, with the increasing \mathcal{F} , the directed flow

becomes larger and the elliptic flow becomes smaller as expected. Both the v_1 and v_2 obtained with the FU3FP1 parametrization and $\mathcal{F} = 0.3$ are close to each other at low p_t , but the difference steadily increases with increasing p_t . It is known that particles with high p_t usually emit early and experience only a few collisions and with a larger relative momentum. The medium correction factor obtained with the FU3FP1 parametrization maintains the momentum dependence, so that the medium suppression effect is weakened at high momenta. Thus the number of collision for the case of the FU3FP1 parametrization is larger than that for $\mathcal{F} = 0.3$. It implies that the collective flow at high transverse momenta would be a promising probe for investigating the medium correction on the NN cross section.

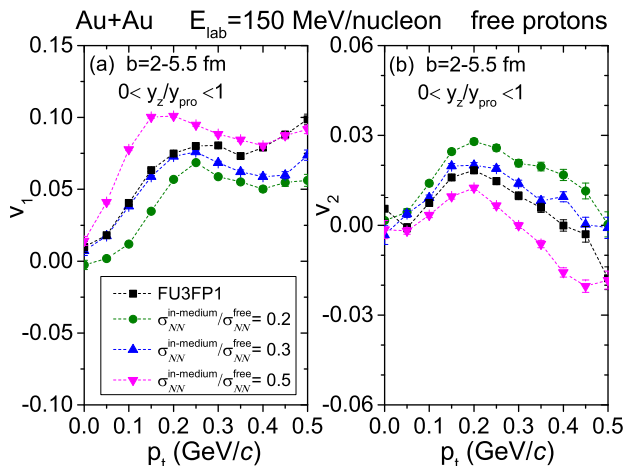


FIG. 4: (Color online) The directed flow v_1 (left) and elliptic flow v_2 (right) of free protons for $^{197}\text{Au} + ^{197}\text{Au}$ collisions at the beam energy 150 MeV/nucleon, as a function of transverse momentum p_t . The impact parameter $b = 2 - 5.5$ fm and the rapidity cut $0 < y_z/y_{p,pro} < 1$ are chosen for both v_1 and v_2 .

B. Nuclear stopping

Besides the collective flow, the degree of nuclear stopping in HICs is another important observable which is also sensitive to the medium correction on the NN cross section [25, 28, 29, 44]. In this work, we calculated the two quantities R_E and $vartl$ from the same reaction. Fig. 5 displays the yield distributions of free protons as functions of the reduced longitudinal and transverse rapidities for central $^{197}\text{Au} + ^{197}\text{Au}$ collisions at $E_{lab} = 40$ (left) and 150 MeV/nucleon (right). And, the FU3FP1 parametrization (top) and $\mathcal{F} = 0.3$ (bottom) are selected for comparison. The extracted values of $vartl$ and R_E are also given in each panel, and they are almost equal to each other at each beam energy as well as with both medium correction factors. We have checked that, although the values of $vartl$ and R_E for free nucleons are almost equal to each other, the values of R_E are usually

smaller than $vartl$ for light fragments such as deuterons and tritons. Further, at $E_{lab} = 40$ MeV/nucleon, the $vartl$ or R_E obtained from the FU3FP1 parametrization are almost the same as that obtained with $\mathcal{F} = 0.3$, while at $E_{lab} = 150$ MeV/nucleon, the values of $vartl$ and R_E obtained from the FU3FP1 are about 14% larger than that from $\mathcal{F} = 0.3$.

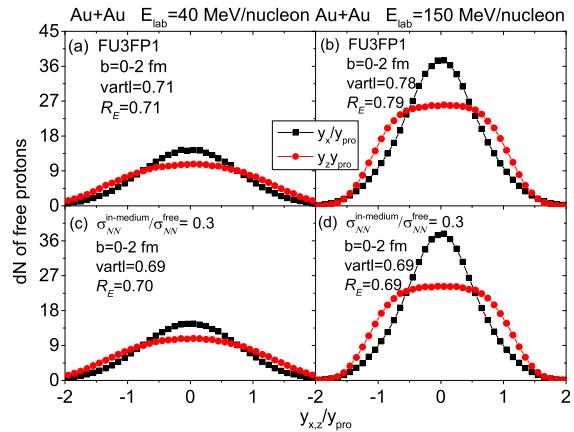


FIG. 5: (Color online) Yield distributions of free protons as functions of the reduced longitudinal ($y_z/y_{p,pro}$, circles) and transverse ($y_x/y_{p,pro}$, squares) rapidities from central ($b = 0-2$ fm) $^{197}\text{Au} + ^{197}\text{Au}$ collisions at $E_{lab} = 40$ (left panels) and 150 (right panels) MeV/nucleon. Calculations with the FU3FP1 parametrization [(a) and (b)] and $\mathcal{F} = 0.3$ [(c) and (d)] are shown. The corresponding values for $vartl$ and R_E are also indicated in each panel.

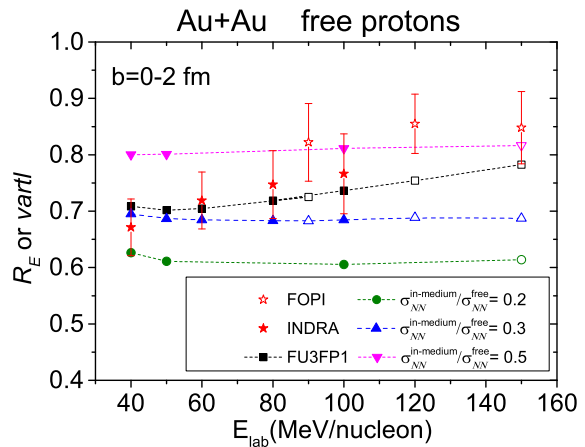


FIG. 6: (Color online) Beam energy dependence of the R_E (solid symbols) and $vartl$ (open symbols) for free protons from central $^{197}\text{Au} + ^{197}\text{Au}$ collisions. Calculations with four different medium correction factors (dashed lines with different symbols) are compared with the FOPI (open stars) and INDRA (solid stars) experimental data, which are taken from Ref. [57] and Ref. [39], respectively.

Fig.6 displays the degree of nuclear stopping (R_E or

$vartl$) in central Au+Au collisions as a function of the beam energy. The results obtained with $\mathcal{F} = 0.5$ are the largest (keep almost constant at ~ 0.8) and those with $\mathcal{F} = 0.2$ are the smallest (~ 0.6) of all. Again, this result from the nuclear stopping observables also consistently supports that the medium correction factors of about 0.2 and 0.5 are required for reasonably describing the degree of nuclear stopping in HICs at $E_{\text{lab}} = 40$ and 150 MeV/nucleon, respectively. Further, the difference between the results from the FU3FP1 parametrization and from $\mathcal{F} = 0.3$ (keep almost constant at ~ 0.7) steadily increases with increasing beam energy. Calculations with FU3FP1 fit the experimental data quite well and reproduce the slightly increased stopping power with increasing beam energy, while others fail to reproduce the observed beam-energy dependence.

IV. SUMMARY

Within the UrQMD model, the effects of the medium correction on the NN elastic cross section on the collective flow and nuclear stopping in Au+Au at beam energies of 40-150 MeV/nucleon are investigated. Calculations performed with the medium correction factor $\mathcal{F} = \sigma_{NN}^{\text{in-medium}}/\sigma_{NN}^{\text{free}}$ of 0.2, 0.3, 0.5, and with the density- and momentum- dependent factor obtained from the FU3FP1 parametrization are compared to the FOPI and INDRA experimental data. It is found that, at E_{lab}

= 40 MeV/nucleon, the slope of the directed flow, the elliptic flow, as well as the nuclear stopping power ($vartl$ and R_E) can be well reproduced with calculations using $\mathcal{F}=0.2$, while $\mathcal{F}=0.5$ is required to reproduce these data at $E_{\text{lab}}=150$ MeV/nucleon. These findings are consistent with the results deduced from the stopping data of protons by the INDRA collaboration. In addition, both the directed and elliptic flow parameters obtained with the FU3FP1 parametrization and $\mathcal{F}=0.3$ are quite close to each other, and sizable difference appears only at high transverse momenta. In general, calculations with the FU3FP1 parametrization fit the FOPI and INDRA data of both the collective flow and the nuclear stopping well, including their beam-energy dependence, while calculations with $\mathcal{F}=0.2, 0.3$, and 0.5 exhibit almost constant degree of stopping in Au+Au with beam energies increasing from 40 to 150 MeV/nucleon.

Acknowledgments

The authors acknowledge the support of the computing server C3S2 at the Huzhou University. This work is supported in part by the National Natural Science Foundation of China (Nos. 11505057, 11375062, 11605270, 11675066, and 11747312), and the Zhejiang Provincial Natural Science Foundation of China (No. LY18A050002).

-
- [1] V. Baran, M. Colonna, V. Greco, and M. Di Toro, Phys. Rept. **410**, 335 (2005).
- [2] A. W. Steiner, M. Prakash, J. M. Lattimer, and P. J. Ellis, Phys. Rept. **411**, 325 (2005).
- [3] J. M. Lattimer and M. Prakash, Phys. Rept. **442**, 109 (2007).
- [4] B. A. Li, L. W. Chen, C. M. Ko, Phys. Rep. **464**, 113 (2008); B. A. Li, A. Ramos, G. Verde, I. Vidana, Eur. Phys. J. A **50**, 9 (2014).
- [5] M. Di Toro, V. Baran, M. Colonna, and V. Greco, J. Phys. G **37**, 083101 (2010).
- [6] E. Khan and J. Margueron, Phys. Rev. C **88**, 034319 (2013); E. Khan and J. Margueron, Phys. Rev. Lett. **109**, 092501 (2012).
- [7] J. R. Stone, N. J. Stone and S. A. Moszkowski, Phys. Rev. C **89**, 044316 (2014).
- [8] A. Le Fèvre, Y. Leifels, W. Reisdorf, J. Aichelin and C. Hartnack, Nucl. Phys. A **945**, 112 (2016).
- [9] Y. J. Wang, C. C. Guo, Q. F. Li, A. Le Fèvre, Y. Leifels, W. Trautmann, Phys. Lett. B **778**, 207-212 (2018)
- [10] G. Q. Li and R. Machleidt, Phys. Rev. C **48**, 1702 (1993); G. Q. Li and R. Machleidt, Phys. Rev. C **49**, 566 (1994).
- [11] F. Sammarruca and P. Krastev, Phys. Rev. C **73**, 014001 (2006).
- [12] H. J. Schulze, A. Schnell, G. Ropke, and U. Lombardo, Phys. Rev. C **55**, 3006 (1997).
- [13] C. Fuchs, A. Faessler, and M. El-Shabshiry, Phys. Rev. C **64**, 024003 (2001).
- [14] H. F. Zhang, Z. H. Li, U. Lombardo, P. Y. Luo, F. Sammarruca, and W. Zuo, Phys. Rev. C **76**, 054001 (2007); H. F. Zhang, U. Lombardo, and W. Zuo, Phys. Rev. C **82**, 015805 (2010).
- [15] W. G. Love and M. A. Franey, Phys. Rev. C **24**, 3 (1981).
- [16] T. Alm, G. Röpke, W. Bauer, F. Daffin and M. Schmidt, Nucl. Phys. A **587**, 815 (1995).
- [17] G. J. Mao, Z. X. Li, Y. Z. Zhuo and Z. Q. Yu, Phys. Lett. B **327**, 183 (1994); G. J. Mao, Z. X. Li, Y. Z. Zhuo, Y. Han and Z. Yu, Phys. Rev. C **49**, 3137 (1994).
- [18] Q. F. Li, Z. X. Li and G. J. Mao, Phys. Rev. C **62**, 014606 (2000); Q. F. Li, Z. X. Li and E. G. Zhao, Phys. Rev. C **69**, 017601 (2004); Q. F. Li and Z. X. Li, Phys. Lett. B **773**, 557 (2017).
- [19] H. M. Xu, Phys. Rev. C **46**, R389 (1992).
- [20] G. D. Westfall *et al.*, Phys. Rev. Lett. **71**, 1986 (1993).
- [21] B. A. Li and A. T. Sustich, Phys. Rev. Lett. **82**, 5004 (1999).
- [22] D. J. Magestro, W. Bauer and G. D. Westfall, Phys. Rev. C **62**, 041603 (2000).
- [23] J. Y. Liu, W. J. Guo, S. J. Wang, W. Zuo, Phys. Rev. Lett. **86**, 975 (2001).
- [24] D. Persram and C. Gale, Phys. Rev. C **65**, 064611 (2002).
- [25] T. Gaitanos, C. Fuchs, and H. H. Wolter, Phys. Lett. B **609**, 241 (2005).
- [26] B. A. Li, P. Danielewicz and W. G. Lynch, Phys. Rev. C **71**, 054603 (2005); B. A. Li and L. W. Chen, Phys. Rev. C **72**, 064611 (2005).

- [27] Q. F. Li, Z. X. Li, S. Soff, M. Bleicher, and H. Stöcker, *J. Phys. G: Nucl. Part. Phys.* **32** 407 (2006).
- [28] Y. X. Zhang, Z. X. Li, *Phys. Rev. C* **74**, 014602 (2006); Y. X. Zhang, Z. X. Li and P. Danielewicz, *Phys. Rev. C* **75**, 034615 (2007).
- [29] Y. Yuan, Q. F. Li, Z. X. Li, and F. H. Liu, *Phys. Rev. C* **81**, 034913 (2010).
- [30] D. D. S. Coupland, W. G. Lynch, M. B. Tsang, P. Danielewicz, Y. X. Zhang, *Phys. Rev. C* **84**, 054603 (2011).
- [31] G. Q. Zhang, Y. G. Ma, X. G. Cao, C. L. Zhou, X. Z. Cai, D. Q. Fang, W. D. Tian and H. W. Wang, *Phys. Rev. C* **84**, 034612 (2011).
- [32] Z. Q. Feng, *Phys. Rev. C* **85**, 014604 (2012).
- [33] Y. X. Zhang, D. D. S. Coupland, P. Danielewicz, Z. X. Li, H. Liu, F. Lu, W. G. Lynch, and M. B. Tsang, *Phys. Rev. C* **85**, 024602 (2012).
- [34] M. Kaur and S. Gautam, *J. Phys. G* **43**, 2, 025103 (2016).
- [35] J. Su *et al.*, *Eur. Phys. J. A* **52**, 207 (2016).
- [36] K. Zbiri, A. Le Fèvre, J. Aichelin *et al.*, *Phys. Rev. C* **75**, 034612 (2007).
- [37] J. Aichelin, *Phys. Rept.* **202**, 233 (1991).
- [38] G. F. Bertsch and S. Das Gupta, *Phys. Rept.* **160**, 189 (1988).
- [39] O. Lopez, D. Durand, G. Lehaut, B. Borderie, J. D. Frankland, M. F. Rivet, R. Bougault, A. Chbihi, E. Galichet, D. Guinet, M. La Commara, N. Le Neindre, I. Lombardo, L. Manduci, P. Marini, P. Napolitani, M. Parlog, E. Rosato, G. Spadaccini, E. Vient, and M. Vigilante (INDRA Collaboration), *Phys. Rev. C* **90**, 064602 (2014).
- [40] B. Rubina, K. Mandeep and K. Suneel, *Indian J. Phys.* **89** 967 (2015).
- [41] Z. Basrak, P. Eudes, and V. de la Mota, **93**, 054609 (2017).
- [42] H. L. Liu, Y. G. Ma, A. Bonasera, X. G. Deng, and O. Lopez, O. and M. Veselský, *Phys. Rev. C* **96**, 064604 (2017).
- [43] Y. Z. Xing, H. F. Zhang, X. B. Liu, Y. M. Zheng, *Nucl. Phys. A* **957** 135 (2017).
- [44] Q. F. Li, C. W. Shen, C. C. Guo, Y. J. Wang, Z. X. Li, J. Lukasik, and W. Trautmann, *Phys. Rev. C* **83**, 044617 (2011).
- [45] Y. J. Wang, C. C. Guo, Q. F. Li, H. F. Zhang, Y. Leifels, and W. Trautmann, *Phys. Rev. C* **89**, 044603 (2014); Y. J. Wang, C. C. Guo, Q. F. Li, H. F. Zhang, Z. X. Li, and W. Trautmann, *Phys. Rev. C* **89**, 034606 (2014); Y. J. Wang, C. C. Guo, Q. F. Li, Z. X. Li, J. Su and H. F. Zhang, *Phys. Rev. C* **94**, 024608 (2016).
- [46] Q. F. Li, Z. X. Li, S. Soff, M. Bleicher and H. Stoecker, *J. Phys. G* **32**, 151 (2006).
- [47] S. A. Bass, M. Belkacem, M. Bleicher, M. Brandstetter, L. Bravina, C. Ernst, L. Gerland and M. Hofmann *et al.*, *Prog. Part. Nucl. Phys.* **41**, 255 (1998).
- [48] C. Hartnack, R. K. Puri, J. Aichelin, J. Konopka, S. A. Bass, H. Stoecker and W. Greiner, *Eur. Phys. J. A* **1**, 151 (1998).
- [49] Y. J. Wang, C. C. Guo, Q. F. Li and H. F. Zhang, *Eur. Phys. J. A* **51**, 37 (2015).
- [50] W. Reisdorf *et al.*, *Nucl. Phys. A* **876**, 1 (2012).
- [51] G. Lehaut *et al.*, *Phys. Rev. Lett.* **104**, 232701 (2010).
- [52] H. Kruse, B. V. Jacak, J. J. Molitoris, G. D. Westfall, and H. Stöcker, *Phys. Rev. C* **31**, 1770 (1985).
- [53] P. Russotto, P. Z. Wu, M. Zoric, M. Chartier, Y. Leifels, R. C. Lemmon, Q. F. Li, J. Lukasik, A. Pagano, P. Pawlowski, and W. Trautmann, *Phys. Lett. B* **697**, 471 (2011).
- [54] Q. F. Li, Y. J. Wang, X. B. Wang, and C. W. Shen, *Sci. China-Phys. Mech. Astron.* **59**, 672013 (2016); *ibid.* **59**, 632002 (2016); *ibid.* **59**, 622001 (2016).
- [55] Y. X. Zhang, Z. X. Li, C. S. Zhou and M. B. Tsang, *Phys. Rev. C* **85**, 051602 (2012).
- [56] A. Andronic, J. Lukasik, W. Reisdorf, and W. Trautmann, *Eur. Phys. J. A* **30**, 31 (2006).
- [57] W. Reisdorf *et al.*, (FOPI Collaborations), *Nucl. Phys. A* **848** 366 (2010).
- [58] S. Kumar and Y. Ma, *Nucl. Sci. Tech.* **24**, no. 5, 50509 (2013).